


Memories of quenches in operator mixing

Joydeep Chakraborty,^{*} Diptarka Das,[†] Bidyut Dey[‡],[§] Suraj Prakash[‡],[§] and Shakeel Ur Rahaman[‡]^{||}
Indian Institute of Technology—Kanpur, Kanpur 208016, Uttar Pradesh, India

 (Received 12 August 2022; accepted 19 October 2022; published 14 November 2022)

We work perturbatively with an interacting quantum field theory comprised of two distinct scalar fields. In this theory, we introduce a sudden quench of the mass of one of the scalars at time t_0 . Also, the quartic interaction between the two scalars is turned on at time t_{in} . These break time-translation invariance. In this setup we examine the effects of the relative ordering of t_0 and t_{in} on composite operator mixing. We study how such operator mixing affects features of the scalar potential. We find that the late time effective potential can be sensitive enough to the quenches to trigger phase transitions.

DOI: [10.1103/PhysRevD.106.105012](https://doi.org/10.1103/PhysRevD.106.105012)

I. INTRODUCTION

We exist *out of equilibrium*, yet most physics tools are mostly developed keeping in mind equilibrium scenarios. Our universe is expanding and hence the quantum fluctuations on top of it are essentially describable via time-dependent couplings which drive the theory into nonequilibrium regimes [1,2]. This is the regime of quantum quenches. The effective field theory is described by the finite set of operators which are commensurate with the symmetries, and in equilibrium, one has the luxury of Poincaré invariance: which limits operators to local ones. However, when the high energy theory becomes subjected to nonequilibrium (as with time-dependent couplings arising in an expanding spacetime) then one does not have time translation symmetry, and the effective theory is no longer local.

The quantum quench, which specifies the time dependence of the couplings can either be sudden or smooth with a characteristic timescale. The physics of quenches have recently garnered a lot of attention in condensed matter systems due to controllable cold atom experiments. In these set-ups critical quenches have been carried out which result in universal scalings as predicted by Kibble and Zurek [3,4]. There are very few analytically tractable examples for KZ scalings and hence most studies have been limited to either free field theories [5–9] or exactly solvable large N

models [10,11], or holographic setups [12]. The mechanisms for these scalings are still poorly understood since they focus on observables which are strongly theory dependent. The observables for time-dependent systems are correlation functions instead of scattering amplitudes, since unlike in a time-translation invariant system the S-matrix is not definable.

In this work, we look at the structure of composite operators in the nonequilibrium theory and try to draw universal lessons. In particular, we consider a generically interacting theory whose couplings are quenched independently. This essentially excites the system, taking us away from adiabaticity. Therefore, in this setting even if we want to integrate out certain heavy field loops, we cannot completely get rid of them from the effective low energy theory. This is because the excitement caused due to the quench also creates heavy field excitations, which are part of the *in*-state [13]. Hence, the time-evolving light field operators, which are now computed using the Schwinger-Keldysh contour [14] or the *in-in* formalism, involve the creation and annihilation of heavy fields. There is a nontrivial operator mixing which contains detailed information about the quench. There are new types of divergences involving time derivatives of the quenched couplings, and RG flows due to a particular quench may trigger quench protocols of other couplings at different scales [15]. Renormalization in the presence of time-dependent couplings also arises in the general case of QFT in curved spacetime as explored in [16–19].

Such operator mixings have previously also been explored in the context of the interacting double scalar ($g^2\phi^2\chi^2$) model [20]. The interaction gets turned on at a particular time t_{in} , which is how the system is driven into nonequilibrium. The authors found by looking into *in-in* correlators that the $\phi^2(t, x)$ operator (at leading order in interaction coupling) mixes with $\chi^2(t)$ as well as with $\chi^2(t_{in})$. However, the renormalization group conditions can

^{*}joydeep@iitk.ac.in

[†]didas@iitk.ac.in

[‡]bidyutd@iitk.ac.in

[§]surajprk@iitk.ac.in

^{||}shakel@iitk.ac.in

Published by the American Physical Society under the terms of the [Creative Commons Attribution 4.0 International license](https://creativecommons.org/licenses/by/4.0/). Further distribution of this work must maintain attribution to the author(s) and the published article's title, journal citation, and DOI. Funded by SCOAP³.

be chosen in a way such that the $\chi^2(t)$ mixing vanishes at the one loop order, though there is no way to get rid of $\chi^2(t_{\text{in}})$ from the mixing. This latter mixing is a signature of *memory* of the quench event. The coefficient of this term, the kernel $K(t - t_{\text{in}})$, is explicitly nonlocal, and shows a power law decay in $m_\phi(t - t_{\text{in}})$, where m_ϕ is the mass of the ϕ field. At very late-times, with proper RG conditions, there is therefore no nontrivial mixing [at $\mathcal{O}(g^2)$], and hence no tell-tale signatures of the quench in the relevant effective potential. In the setup of our present work, we work with the same double scalar model, however, making departures in two different directions:

- (1) We introduce a mass quench in one of the fields. This is done independently from the interaction quench, viz. the mass quench occurs at some time t_0 which is generically different from the time of the interaction quench.
- (2) The effect of the mass quench is treated nonperturbatively. This is both important (as the mass operator is more relevant) as well as possible (as the time-dependent free theory is still quadratic).

Our results show a variety of interesting features, some of which we summarize below:

- (1) There is memory of both the quench events: the mass quench as well as the interaction quench in the operator mixing. In the composite operator $\phi^2(t, \vec{x})$ the signature of this is the presence of $\chi^2(t_{\text{in}})$ which comes with its own nonlocal memory kernels. The kernels are different depending on the order of the quenches. However, both these kernels decay at large times away from the quench events and hence disappear from late-time perturbative physics. The presence of memory right after the quench is a signature of the deep non-Markovian characteristic of nonequilibrium QFT [21].
- (2) As with the interaction quench, we once again have the mixing with the local operator: $\chi^2(t)$. However, unlike [20], this time there is no RG condition which can make this go away. This is because, in addition to the logarithmic divergence, the coefficient also contains finite terms arising purely due to the mass quench. This term, therefore, affects late-time physics. Thus, the signatures get carried over into the effective potential, and hence these very early-time quenches can play a crucial role in deciding the late-time phase structure of the quantum field configuration. This possibility is very tantalizing when put in the context of quantum fluctuations during inflation.

We would like to clarify that the main reason we have investigated sudden quenches rather than smooth ones, is due to technical advantage rather than a physical one, as a renormalizable theory comes with an UV cutoff. However the sudden quench allows for an exact determination of the nonequilibrium propagators as the initial state is an uncorrelated one. On the other hand, only certain smooth

quench protocols can be treated exactly, else one has to use either adiabatic perturbation theory, or linear response/Kubo formula which does not allow for extracting time physics.

In the sections to follow, we proceed with the following outline: In Sec. II we work out the nonequilibrium Greens function for a time-dependent quantum harmonic oscillator. This will directly apply to the scalar field theory with the mass quench and will allow us to determine the free propagators along the Keldysh contours. Section III introduces the model that we focus on and the quench protocols. After defining the Feynman rules on the Keldysh contour, we proceed in this section to compute the one loop effect of the interaction on operator mixings for the different quench sequences. Next in Sec. IV we discuss the renormalization and late-time analytical form of the perturbative mixing. We also evaluate various contributions to the composite operator numerically and point out crucial dependencies on the details of the quench protocol. Section V deals with the impact of the nontrivial mixing on the effective potential and explicitly analyzes how the mass quench can affect the late-time phase diagram of the theory. We end with conclusions in Sec. VI.

II. SIMPLE HARMONIC OSCILLATOR WITH TIME DEPENDENT HAMILTONIAN

In momentum space, the free scalar field theory is a set of independent quantum harmonic oscillators. We will need the nonequilibrium Green's functions for the free scalar field due to mass quench. Hence, in this section, we compute the analogous correlators for the single oscillator, which we will employ to compute the Green's functions for the free scalar field. If the frequency of a simple harmonic oscillator is suddenly quenched from ω_0 to ω at time $t = t_0$ [22,23], then its Hamiltonian carries an explicit time-dependence which can be described as

$$H(t) = \frac{1}{2} p^2 + \frac{\omega^2(t)}{2} q^2, \quad (2.1)$$

with $\omega^2(t) = \theta(t_0 - t)\omega_0^2 + \theta(t - t_0)\omega^2$. The time dependence is captured within the Heaviside theta functions. Away from t_0 , the Hamiltonian in each region (for $t < t_0$ as well as for $t > t_0$) assumes the usual time-independent form, but with different frequencies (ω_0 for $t < t_0$ and ω for $t > t_0$) in the two regions. Therefore, the initial Hamiltonian before quench ($t < t_0$) is

$$H_{\text{in}} = \frac{1}{2} p^2 + \frac{1}{2} \omega_0^2 x^2.$$

In the Heisenberg picture, the time evolution of position operator x for $t < t_0$ can be expressed in terms of creation and annihilation operators, a_{in}^\dagger and a_{in} , as

$$x(t < t_0) = \frac{1}{\sqrt{2\omega_0}} (e^{-i\omega_0(t-t_0)} a_{\text{in}} + e^{i\omega_0(t-t_0)} a_{\text{in}}^\dagger), \quad (2.2)$$

where the annihilation operator acts on the ground state configuration of the initial states to give 0, i.e., $a_{\text{in}}|0_{\text{in}}\rangle = 0$. This allows us to recast the Hamiltonian as

$$H_{\text{in}} = \left(a_{\text{in}}^\dagger a_{\text{in}} + \frac{1}{2} \right) \omega_0. \quad (2.3)$$

The expression for the final Hamiltonian, after the quench ($t > t_0$), is given as

$$H_{\text{out}} = \frac{1}{2} p^2 + \frac{1}{2} \omega^2 x^2.$$

Once again, the Heisenberg picture position operator in $t > t_0$ can again be expressed as

$$x(t > t_0) = \frac{1}{\sqrt{2\omega}} (e^{-i\omega(t-t_0)} a_{\text{out}} + e^{i\omega(t-t_0)} a_{\text{out}}^\dagger), \quad (2.4)$$

where $a_{\text{out}}|0_{\text{out}}\rangle = 0$ since $|0_{\text{out}}\rangle$ is the ground state of the final Hamiltonian. It is obvious that $|0_{\text{in}}\rangle \neq |0_{\text{out}}\rangle$. H_{out} can be rewritten in terms of a_{out}^\dagger and a_{out} as

$$H_{\text{out}} = \left(a_{\text{out}}^\dagger a_{\text{out}} + \frac{1}{2} \right) \omega. \quad (2.5)$$

When $\omega_0 = \omega$ then $a_{\text{in}} = a_{\text{out}}$, otherwise they are different. However using a Bogoliubov transformation one can recast a_{out} as a linear combination of a_{in} and a_{in}^\dagger as shown below:

$$a_{\text{out}} = A_1 a_{\text{in}} + A_2 a_{\text{in}}^\dagger. \quad (2.6)$$

We compute the Bogoliubov coefficients by matching the Heisenberg operators at quench time t_0 . Explicit computation of the Bogoliubov coefficients yields [23]:

$$A_1 = \frac{\omega - \omega_0}{2\sqrt{\omega\omega_0}}, \quad A_2 = \frac{\omega + \omega_0}{2\sqrt{\omega\omega_0}}. \quad (2.7)$$

Using the above result to replace $A_{1,2}$ by coefficients dependent on ω_0 and ω in Eq. (2.6) and substituting for a_{out} in Eq. (2.4) we get,

$$x(t > t_0) = [u_{\text{in}}(t) a_{\text{in}} + u_{\text{in}}^*(t) a_{\text{in}}^\dagger], \quad (2.8)$$

with,

$$u_{\text{in}}(t) = \frac{1}{\sqrt{2\omega_0}} \left[\cos(\omega(t-t_0)) - \frac{i\omega_0}{\omega} \sin(\omega(t-t_0)) \right]. \quad (2.9)$$

Combining the position operators, see Eqs. (2.2) and (2.8) for the two regions ($t < t_0$ and $t > t_0$) using Heaviside θ -functions we obtain,

$$x(t) = \left(\theta(t_0 - t) \frac{e^{-i\omega_0(t-t_0)}}{\sqrt{2\omega_0}} + \theta(t - t_0) u_{\text{in}}(t) \right) a_{\text{in}} + \left(\theta(t_0 - t) \frac{e^{i\omega_0(t-t_0)}}{\sqrt{2\omega_0}} + \theta(t - t_0) u_{\text{in}}^*(t) \right) a_{\text{in}}^\dagger. \quad (2.10)$$

The expectation value of two position operators at different times t_1 and t_2 in the in-vacuum state takes the form as

$$\begin{aligned} \langle 0_{\text{in}} | x(t_1) x(t_2) | 0_{\text{in}} \rangle &= \left(\theta(t_0 - t_1) \frac{e^{-i\omega_0(t_1-t_0)}}{\sqrt{2\omega_0}} + \theta(t_1 - t_0) u_{\text{in}}(t_1) \right) \\ &\times \left(\theta(t_0 - t_2) \frac{e^{i\omega_0(t_2-t_0)}}{\sqrt{2\omega_0}} + \theta(t_2 - t_0) u_{\text{in}}^*(t_2) \right). \end{aligned} \quad (2.11)$$

It is worth mentioning that always in the limit $\omega = \omega_0$, i.e., for no quench, the above two-point correlation function assumes the same form as the correlation function of the two position operators at different times for a harmonic oscillator with time-independent frequency, i.e.,

$$\langle 0_{\text{in}} | x(t_1) x(t_2) | 0_{\text{in}} \rangle = \frac{1}{2\omega} e^{-i\omega(t_1-t_2)}. \quad (2.12)$$

III. COMPOSITE OPERATOR MIXING THROUGH (NON)LOCAL KERNELS

As alluded to in the introduction, the operator correlators are the observables in the *in-in* formalism. In a quantum field theory, there are infinite operators which can be organized in scales of relevance. Among the members of this infinite set, the composite operator built by squaring the fundamental field: $\phi^2(t, \vec{x})$, is the simplest nontrivial one, which contributes to the energy. In an interacting QFT this operator generically exhibits nontrivial mixing with other fundamental fields in the theory. This arises when, in the connected Feynman diagrams involving ϕ^2 , there are loops consisting of the other fundamental fields. Clearly this originates due to interaction between the different fundamental fields, and usually results in nontrivial renormalization group flow of the composite operator. The flow decides among other things the measurable critical exponents associated with various physical observables where ϕ^2 contributes. It is far from understood how

operator mixing takes place in *out of equilibrium*. In what follows, we have studied the mixing of ϕ^2 in systems where time-translation invariance is broken explicitly by multiple quantum quenches.

A. Model description and Green's functions

We consider a simplified framework consists of two real scalar fields ϕ and χ with different mass parameters, and the Lagrangian for the system can be written as

$$\mathcal{L} = \mathcal{L}_0[\phi, \chi] + \mathcal{L}_{\text{int}}[\phi, \chi] - \frac{\lambda_\phi}{4!} \phi^4 - \frac{\lambda_\chi}{4!} \chi^4, \quad (3.1)$$

where \mathcal{L}_0 describes the free-field Lagrangian and \mathcal{L}_{int} encapsulates the interaction between the two fields, i.e.,

$$\begin{aligned} \mathcal{L}_0[\phi, \chi] &= \frac{1}{2}(\partial_\mu \phi \partial^\mu \phi) - \frac{1}{2}m^2(t)\phi^2 + \frac{1}{2}(\partial_\mu \chi \partial^\mu \chi) - \frac{1}{2}M^2\chi^2, \\ \mathcal{L}_{\text{int}}[\phi, \chi] &= -\frac{g^2}{2}\phi^2\chi^2. \end{aligned} \quad (3.2)$$

The only internal symmetry respected by the Lagrangian is a \mathbb{Z}_2 symmetry for each of the fields that filters out terms containing odd powers of either field from the Lagrangian. Terms such as quartic self-interaction of the fields does not contribute in the operator mixing of ϕ^2 but will be of significance when the impact of composite operator mixing on the scalar potential is discussed. Also, the term linear in both fields, i.e., the $\phi\chi$ coupling can be removed through global rotations of the two fields followed by field redefinitions.

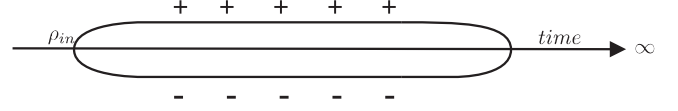


FIG. 1. Closed time contour \mathcal{C} .

The breaking of time-translation invariance has been accomplished in two ways:

- (1) By imposing an explicit initial time t_{in} as the lower limit of the time integral present in the path integral. Since we are looking at the composite operator ϕ^2 , this is equivalent to quenching the interaction term by suddenly turning on the interaction at time $t = t_{\text{in}}$ [20]. Based on this, one can write the action as,

$$\begin{aligned} S[\phi, \chi] &= \int_{-\infty}^{\infty} dt \int d^3x (\mathcal{L}_0[\phi, \chi] \\ &+ \Theta(t - t_{\text{in}}) \mathcal{L}_{\text{int}}[\phi, \chi]). \end{aligned} \quad (3.3)$$

- (2) Additionally, we suddenly change the mass of the ϕ field from m_0 to m at a time $t = t_0$ which we have referred to as the mass quench of the scalar field throughout the paper.

The breaking of time-translation invariance prompts us to follow the Schwinger-Keldysh (or the *in-in*) formulation. This results in doubling the degrees of freedom for both $\phi(x)$ and $\chi(x)$ (through the introduction of $\phi_{\pm}(x)$ and $\chi_{\pm}(x)$). On the Schwinger-Keldysh contour Fig. 1, the action is expressed as:

$$\begin{aligned} S &= \int_{t_{\text{in}}}^{\infty} dt \int d^3x [\mathcal{L}[\phi_+, \chi_+] - \mathcal{L}[\phi_-, \chi_-]] \\ &= \int_{t_{\text{in}}}^{\infty} dt \int d^3x \left[\frac{1}{2}(\partial_\mu \phi_+)(\partial^\mu \phi_+) - \frac{1}{2}m^2\phi_+^2 + \frac{1}{2}(\partial_\mu \chi_+)(\partial^\mu \chi_+) - \frac{1}{2}M^2\chi_+^2 - \frac{g^2}{2}\phi_+^2\chi_+^2 \right. \\ &\quad \left. - \frac{1}{2}(\partial_\mu \phi_-)(\partial^\mu \phi_-) + \frac{1}{2}m^2\phi_-^2 - \frac{1}{2}(\partial_\mu \chi_-)(\partial^\mu \chi_-) + \frac{1}{2}M^2\chi_-^2 + \frac{g^2}{2}\phi_-^2\chi_-^2 \right]. \end{aligned} \quad (3.4)$$

Free scalar field theory can be described as the superposition of independent momentum modes, each of which evolves as a simple harmonic oscillator. Consequently, the propagators of a scalar field and that of a harmonic oscillator can be related by a Fourier transform,

$$\begin{aligned} G_{-+}^\phi(x, y) &= \langle \phi(x)\phi(y) \rangle = \int \frac{d^3\vec{k}}{(2\pi)^3} e^{-i\vec{k}\cdot(\vec{x}-\vec{y})} G_{-+}^\phi(\vec{k}, t_1, t_2), \\ G_{+-}^\phi(x, y) &= \langle \phi(y)\phi(x) \rangle = \int \frac{d^3\vec{k}}{(2\pi)^3} e^{-i\vec{k}\cdot(\vec{x}-\vec{y})} G_{+-}^\phi(\vec{k}, t_1, t_2). \end{aligned} \quad (3.5)$$

Here, $x = (t_1, \vec{x})$, $y = (t_2, \vec{y})$, $t_1 \equiv x^0$ and $t_2 \equiv y^0$. We assume that the initial density matrix ρ_{in} is the vacuum state of free field theory. The Green's functions in the momentum space are expressed as [see Eq. (2.11)]

$$G_{-+}^\phi(\vec{k}, t_1, t_2) = \left(\theta(t_0 - t_1) \frac{e^{-i\omega_0 k(t_1 - t_0)}}{\sqrt{2\omega_0 k}} + \theta(t_1 - t_0) u_{\text{in}}(\vec{k}, t_1) \right) \left(\theta(t_0 - t_2) \frac{e^{i\omega_0 k(t_2 - t_0)}}{\sqrt{2\omega_0 k}} + \theta(t_2 - t_0) u_{\text{in}}^*(\vec{k}, t_2) \right) = G_{+-}^\phi(\vec{k}, t_2, t_1). \quad (3.6)$$

In the above equation, $u_{\text{in}}(\vec{k}, t_i)$ and $u_{\text{in}}^*(\vec{k}, t_i)$, $i = 1, 2$ are the functions defined in Eq. (2.9) with the momentum dependence explicitly highlighted, i.e.,

$$u_{\text{in}}(\vec{k}, t) = \frac{1}{\sqrt{2\omega_{0k}}} \left[\cos(\omega_k(t-t_0)) - \frac{i\omega_{0k}}{\omega_k} \sin(\omega_k(t-t_0)) \right]. \quad (3.7)$$

Here, $\omega_{0k} = \sqrt{\vec{k}^2 + m_0^2}$ and $\omega_k = \sqrt{\vec{k}^2 + m^2}$ are the frequencies of the ϕ field before and after the mass quench. The propagators for χ fields can similarly be written as:

$$\begin{aligned} G_{-+}^{\chi}(x, y) &= \langle \chi(x)\chi(y) \rangle = \int \frac{d^3\vec{k}}{(2\pi)^3} e^{-i\vec{k}\cdot(\vec{x}-\vec{y})} G_{-+}^{\chi}(\vec{k}, t_1, t_2), \\ G_{+-}^{\chi}(x, y) &= \langle \chi(y)\chi(x) \rangle = \int \frac{d^3\vec{k}}{(2\pi)^3} e^{-i\vec{k}\cdot(\vec{x}-\vec{y})} G_{+-}^{\chi}(\vec{k}, t_1, t_2). \end{aligned} \quad (3.8)$$

In this case, the momentum space Green's functions for the χ fields have the following simple form:

$$G_{-+}^{\chi}(\vec{k}, t_1, t_2) = \frac{e^{-i\Omega_k(t_1-t_2)}}{2\Omega_k} = G_{+-}^{\chi}(\vec{k}, t_2, t_1), \quad (3.9)$$

with $\Omega_k = \sqrt{\vec{k}^2 + M^2}$ being the frequency. The time ordered and anti-time ordered propagators of the fields can be expressed respectively by the linear combinations of the Green's functions defined in Eqs. (3.5) and (3.8) as

$$\begin{aligned} G_{++}^{\phi\chi}(x, y) &= \theta(x^0 - y^0) G_{-+}^{\phi\chi}(x, y) + \theta(y^0 - x^0) G_{+-}^{\phi\chi}(x, y), \\ G_{--}^{\phi\chi}(x, y) &= \theta(x^0 - y^0) G_{+-}^{\phi\chi}(x, y) + \theta(y^0 - x^0) G_{-+}^{\phi\chi}(x, y). \end{aligned} \quad (3.10)$$

The Feynman rules corresponding to the ϕ_{\pm} and χ_{\pm} fields, the different propagators of ϕ and χ , $G_{ij}^{\phi\chi}$ fields with $i, j \in \{+, -\}$, and for the vertices of the quartic interactions— $\phi_{\pm}^2\chi_{\pm}^2$ and $\phi_{\pm}^2\chi_{\mp}^2$ have been depicted in Figs. 2–4 respectively.

B. Effect of the chronology of quenches on operator mixing

In [20], an expression for $\phi^2(t)$ in terms of $\chi^2(t)$, $\chi^2(t_0)$, $\chi^2(t_{\text{in}})$ was obtained when time-translation symmetry was broken by explicitly switching on the ϕ - χ quartic interaction at time t_{in} .



FIG. 2. Symbols corresponding to the ϕ_{\pm} , and χ_{\pm} fields.

Here, we outline the effect of introducing a sudden quench of the mass of ϕ field ($m_0 \rightarrow m$) at t_0 in addition to switching on the quartic interaction at t_{in} and highlight the differences between two specific cases—(1.) $t_0 < t_{\text{in}}$ and (2.) $t_{\text{in}} < t_0$.

To obtain the expression for $\phi^2(t)$ in terms of $\chi^2(t)$, $\chi^2(t_0)$, $\chi^2(t_{\text{in}})$, it is necessary to first compute the sum of all possible connected Green's functions of the form $\langle \phi_i(t)\phi_j(t)\chi_k(t_1)\chi_l(t_2) \rangle_c$ (the subscript c denotes connected correlators) with $i, j, k, l \in \{+, -\}$. Thus there will be $2^4 = 16$ different correlation functions. It must be noted that in both the cases taken into account in our analysis: $t_0 < t_{\text{in}}$ or $t_{\text{in}} < t_0$, the other time instances involved in the four-point correlation function $\langle \phi_i(t)\phi_j(t)\chi_k(t_1)\chi_l(t_2) \rangle_c$, i.e., t, t_1, t_2 always maintain the chronology $t_0, t_{\text{in}} < t < t_1 < t_2$. We restrict ourselves to the cases with $t > t_0, t_{\text{in}}$ because we are interested in late-time physics. Also, $t_1, t_2 > t$ must hold so that there is no effect of the external states on the operator mixing.

We commence by first computing $\langle \phi_{\pm}^2(t)\chi_{\pm}(t_1)\chi_{\pm}(t_2) \rangle_c$. At order $\mathcal{O}(g^2)$, it receives contributions from the one-loop diagrams L_1 and L_2 shown in Fig. 5. Two additional diagrams, L'_1 and L'_2 which differ from L_1 and L_2 only with respect to the exchange $\vec{p}_1 \leftrightarrow \vec{p}_2$ also contribute to this

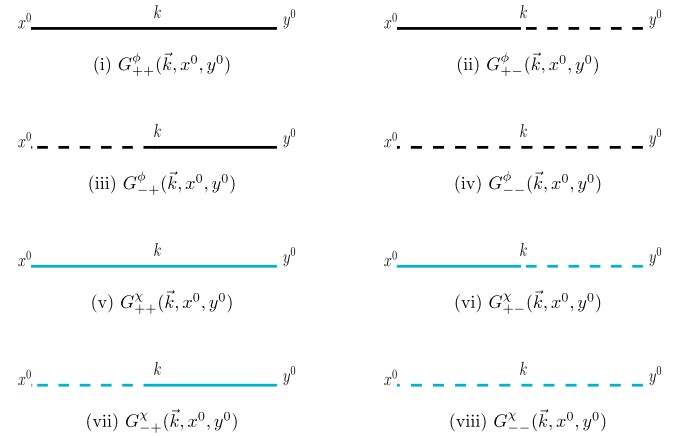


FIG. 3. Diagrammatic representation of Green's functions $G_{ij}^{\phi\chi}(x^0, y^0)$ with $i, j \in \{+, -\}$.

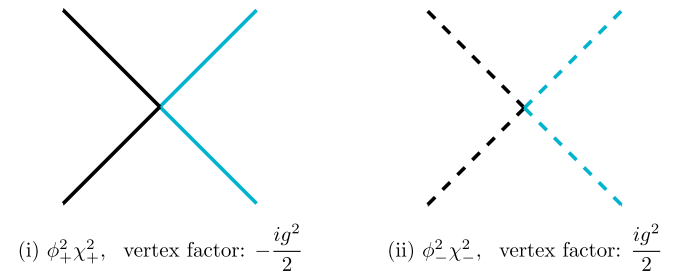


FIG. 4. Feynman diagrams corresponding to contact interactions.

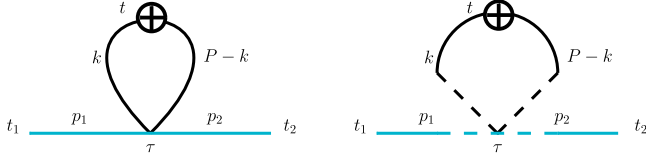


FIG. 5. One-loop diagrams (i) L_1 and (ii) L_2 that contribute to the four-point correlation function $\langle \phi_+^2(t) \chi_+(t_1) \chi_+(t_2) \rangle_c$ at order $O(g^2)$. The \oplus denotes the composite operator $\phi_+^2(t)$.

correlation function. A detailed description of the loop calculations has been summarized in Appendix A. In the calculations shown below, we delve into the explicit details for only $\langle \phi_+^2(t) \chi_+(t_1) \chi_+(t_2) \rangle_c$, for the other 15 correlation functions $\langle \phi_i(t) \phi_j(t) \chi_k(t_1) \chi_l(t_2) \rangle_c$ similar steps must be followed. It must be emphasized that each of the other 15 correlation functions can be calculated using diagrams similar to L_1, L_2 (along with their momentum-exchanged ($\vec{p}_1 \leftrightarrow \vec{p}_2$) counterparts).

1. Case 1: $t_0 < t_{in} \leq t < t_1 < t_2$, Fig. 6

The leading order term on the right hand side for $\langle \phi_+^2(t) \chi_+(t_1) \chi_+(t_2) \rangle_c$ in this case, obtained after evaluating the time integrals in the calculation of loop diagrams, see

$$L_1 + L_2 + L'_1 + L'_2 = \left(\left[\frac{e^{i\Omega_{p_1}(t_1-t_{in})} e^{i\Omega_{p_2}(t_2-t_{in})}}{2\Omega_{p_1} 2\Omega_{p_2}} \right] c_1(t_{in}, t_0, t) + \left[\frac{e^{-i\Omega_{p_1}(t_1-t_{in})} e^{-i\Omega_{p_2}(t_2-t_{in})}}{2\Omega_{p_1} 2\Omega_{p_2}} \right] c_2(t_{in}, t_0, t) \right. \\ \left. + \left[\frac{e^{i\Omega_{p_1}(t-t_1)} e^{i\Omega_{p_2}(t-t_2)}}{2\Omega_{p_1} 2\Omega_{p_2}} \right] c_3(t_{in}, t_0, t) \right) + \vec{p}_1 \rightarrow \vec{p}_2, \quad (3.11)$$

which implies the following:

$$\langle \phi_+^2(t) \chi_+(t_1) \chi_+(t_2) \rangle_c = \langle \chi_-^2(t_{in}) \chi_+(t_1) \chi_+(t_2) \rangle_c c_1(t_{in}, t_0, t) + \langle \chi_+^2(t_{in}) \chi_+(t_1) \chi_+(t_2) \rangle_c c_2(t_{in}, t_0, t) \\ + \langle \chi_+^2(t) \chi_+(t_1) \chi_+(t_2) \rangle_c c_3(t_{in}, t_0, t). \quad (3.12)$$

Here, the connected four-point correlation functions of χ have been identified as:

$$\langle \chi_-^2(t_{in}) \chi_+(t_1) \chi_+(t_2) \rangle_c = \frac{e^{i\Omega_{p_1}(t_1-t_{in})} e^{i\Omega_{p_2}(t_2-t_{in})}}{2\Omega_{p_1} 2\Omega_{p_2}} + (\vec{p}_1 \rightarrow \vec{p}_2), \\ \langle \chi_+^2(t_{in}) \chi_+(t_1) \chi_+(t_2) \rangle_c = \frac{e^{-i\Omega_{p_1}(t_1-t_{in})} e^{-i\Omega_{p_2}(t_2-t_{in})}}{2\Omega_{p_1} 2\Omega_{p_2}} + (\vec{p}_1 \rightarrow \vec{p}_2), \\ \langle \chi_+^2(t) \chi_+(t_1) \chi_+(t_2) \rangle_c = \frac{e^{i\Omega_{p_1}(t-t_1)} e^{i\Omega_{p_2}(t-t_2)}}{2\Omega_{p_1} 2\Omega_{p_2}} + (\vec{p}_1 \rightarrow \vec{p}_2). \quad (3.13)$$

The time-dependent coefficients are each, in fact, integrals over the momentum \vec{k} , with the integrands being functions of ω_k and ω_{0k} . Absorbing the coupling constant g^2 within these coefficients allows us to write them as:

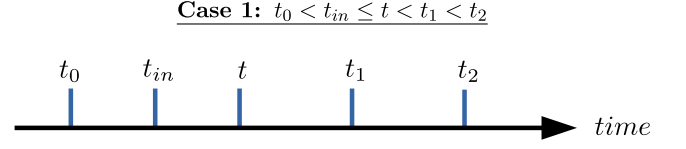


FIG. 6. The chronology of events in the first case. Here, t_0 corresponds to the time when mass quench occurs, t_{in} indicates the time when the interaction between ϕ and χ fields is turned on and t refers to the time of the measurement. t_1, t_2 correspond to the external states.

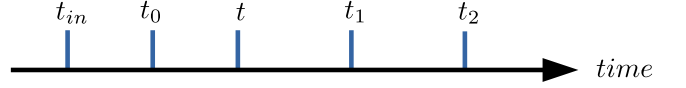


FIG. 7. The chronology of events in the second case. Once again, t_0 corresponds to the time when mass quench occurs, t_{in} indicates the time when the interaction between ϕ and χ fields is turned on and t refers to the time of the measurement. t_1, t_2 correspond to the external states.

Appendix A, is comprised of an integrand of order $1/|\vec{k}|^3$. We can identify four-point correlation functions of χ in the result, each multiplied by a time-dependent coefficient as shown below:

$$\begin{aligned}
c_1(t_{\text{in}}, t_0, t) &= \frac{g^2}{8} \int \frac{d^3 \vec{k}}{(2\pi)^3} \frac{1}{\omega_k^2 \omega_{0k}} \left[\cos \omega_k(t-t_0) + i \frac{\omega_{0k}}{\omega_k} \sin \omega_k(t-t_0) \right]^2 \left[\cos 2\omega_k(t_{\text{in}} - t_0) - i \frac{(\omega_k^2 + \omega_{0k}^2)}{2\omega_k \omega_{0k}} \sin 2\omega_k(t_{\text{in}} - t_0) \right], \\
c_2(t_{\text{in}}, t_0, t) &= \frac{g^2}{8} \int \frac{d^3 \vec{k}}{(2\pi)^3} \frac{1}{\omega_k^2 \omega_{0k}} \left[\cos \omega_k(t-t_0) - i \frac{\omega_{0k}}{\omega_k} \sin \omega_k(t-t_0) \right]^2 \left[\cos 2\omega_k(t_{\text{in}} - t_0) + i \frac{(\omega_k^2 + \omega_{0k}^2)}{2\omega_k \omega_{0k}} \sin 2\omega_k(t_{\text{in}} - t_0) \right], \\
c_3(t_0, t) &= -\frac{g^2}{8} \int \frac{d^3 \vec{k}}{(2\pi)^3} \frac{1}{\omega_k^2 \omega_{0k}} \left[(\cos \omega_k(t-t_0) + i \frac{\omega_{0k}}{\omega_k} \sin \omega_k(t-t_0))^2 \left(\cos 2\omega_k(t-t_0) - i \frac{(\omega_k^2 + \omega_{0k}^2)}{2\omega_k \omega_{0k}} \sin 2\omega_k(t-t_0) \right) \right. \\
&\quad \left. + \left(\cos \omega_k(t-t_0) - i \frac{\omega_{0k}}{\omega_k} \sin \omega_k(t-t_0) \right)^2 \left(\cos 2\omega_k(t-t_0) + i \frac{(\omega_k^2 + \omega_{0k}^2)}{2\omega_k \omega_{0k}} \sin 2\omega_k(t-t_0) \right) \right]. \quad (3.14)
\end{aligned}$$

In the limit of no mass quench, i.e., for $m_0 \rightarrow m$, we, these simplify considerably:

$$\begin{aligned}
c_1(t_{\text{in}}, t_0, t) &\rightarrow \frac{g^2}{8} \int \frac{d^3 \vec{k}}{(2\pi)^3} \frac{1}{\omega_k^3} e^{2i\omega_k(t-t_{\text{in}})}, \\
c_3(t_0, t) &\rightarrow -\frac{2g^2}{8} \int \frac{d^3 \vec{k}}{(2\pi)^3} \frac{1}{\omega_k^3}, \\
c_2(t_{\text{in}}, t_0, t) &\rightarrow \frac{g^2}{8} \int \frac{d^3 \vec{k}}{(2\pi)^3} \frac{1}{\omega_k^3} e^{-2i\omega_k(t-t_{\text{in}})}. \quad (3.15)
\end{aligned}$$

After repeating similar steps for all 16 correlation functions $\langle \phi_i(t) \phi_j(t) \chi_k(t_1) \chi_l(t_2) \rangle_c$ with $i, j, k, l \in \{+, -\}$, summing them and setting $\phi_+ = \phi_- = \phi$, as well as $\chi_+ = \chi_- = \chi$ to return to a description in terms of the physical fields ϕ and χ [20], we find that

$$\begin{aligned}
&\langle \phi^2(t) \chi(t_1) \chi(t_2) \rangle_c \\
&= \underbrace{(c_1(t_{\text{in}}, t_0, t) + c_2(t_{\text{in}}, t_0, t))}_{K_1(t-t_{\text{in}})} \langle \chi^2(t_{\text{in}}) \chi(t_1) \chi(t_2) \rangle_c \\
&\quad + \underbrace{c_3(t_0, t)}_{c_3(t-t_0)} \langle \chi^2(t) \chi(t_1) \chi(t_2) \rangle_c. \quad (3.16)
\end{aligned}$$

The nonlocal and local kernels have been identified as, ignoring terms of $\mathcal{O}(1/|\vec{k}|^5)$:

$$\begin{aligned}
K_1(t-t_{\text{in}}) &= c_1(t_{\text{in}}, t_0, t) + c_2(t_{\text{in}}, t_0, t) \\
&\approx \frac{g^2}{8} \int \frac{d^3 \vec{k}}{(2\pi)^3} \frac{\omega_k^2 + \omega_{0k}^2}{\omega_k^4 \omega_{0k}} \cos(2\omega_k(t-t_{\text{in}})), \quad (3.17)
\end{aligned}$$

$$c_3 \approx -\frac{g^2}{8} \int \frac{d^3 \vec{k}}{(2\pi)^3} \frac{\omega_k^2 + \omega_{0k}^2}{\omega_k^4 \omega_{0k}}. \quad (3.18)$$

The relation between the four-point correlators allows us to write the following relation between composite operators in terms of (non)local kernels:

$$\phi_R^2(t) = \phi^2(t) + K_1(t-t_{\text{in}}) \chi^2(t_{\text{in}}) + c_3 \chi^2(t) + \text{counterterms}. \quad (3.19)$$

In the above, $\phi^2(t)$ arises from the disconnected diagram, where $\phi(t)$ is the bare field. The counterterms are necessary to renormalize the divergence within c_3 . Details pertaining to the renormalization of c_3 as well the features of K_1 have been discussed in Sec. IV.

2. Case 2: $t_{\text{in}} < t_0 < t < t_1 < t_2$, Fig. 7

The leading order term on the right-hand side for $\langle \phi_+^2(t) \chi_+(t_1) \chi_+(t_2) \rangle_c$, obtained after evaluating the time integrals in the calculation of loop diagrams, is once again comprised of integrands of order $1/|\vec{k}|^3$. We proceed in a manner similar to Case 1 by expressing the result as a combination of four-point correlation functions of χ and by studying the behavior of their time-dependent coefficients.

$$\begin{aligned}
L_1 + L_2 + L'_1 + L'_2 &= \left(\left[\frac{e^{i\Omega_{p_1}(t_1-t_{\text{in}})} e^{i\Omega_{p_2}(t_2-t_{\text{in}})}}{2\Omega_{p_1} 2\Omega_{p_2}} \right] c'_1(t_{\text{in}}, t_0, t) \right. \\
&\quad \left. + \left[\frac{e^{-i\Omega_{p_1}(t_1-t_{\text{in}})} e^{-i\Omega_{p_2}(t_2-t_{\text{in}})}}{2\Omega_{p_1} 2\Omega_{p_2}} \right] c'_2(t_{\text{in}}, t_0, t) \right. \\
&\quad \left. + \left[\frac{e^{i\Omega_{p_1}(t-t_1)} e^{i\Omega_{p_2}(t-t_2)}}{2\Omega_{p_1} 2\Omega_{p_2}} \right] c'_3(t_{\text{in}}, t_0, t) \right) \\
&\quad + \vec{p}_1 \rightarrow \vec{p}_2, \quad (3.20)
\end{aligned}$$

which implies the following:

$$\begin{aligned}
\langle \phi_+^2(t) \chi_+(t_1) \chi_+(t_2) \rangle_c &= \langle \chi_-^2(t_{\text{in}}) \chi_+(t_1) \chi_+(t_2) \rangle_c c'_1(t_{\text{in}}, t_0, t) + \langle \chi_+^2(t_{\text{in}}) \chi_+(t_1) \chi_+(t_2) \rangle_c c'_2(t_{\text{in}}, t_0, t) \\
&\quad + \langle \chi_+^2(t) \chi_+(t_1) \chi_+(t_2) \rangle_c c'_3(t_{\text{in}}, t_0, t). \quad (3.21)
\end{aligned}$$

The four-point correlation functions of χ above are the same as the ones defined in Eq. (3.13). The difference between Case 1 and 2 appears within the time-dependent coefficients which for Case 2 are written below:

$$\begin{aligned}
c'_1(t_{\text{in}}, t_0, t) &= \frac{g^2}{8} \int \frac{d^3\vec{k}}{(2\pi)^3} \frac{1}{\omega_{0k}^3} e^{2i\omega_{0k}(t_0-t_{\text{in}})} \left[\cos \omega_k(t-t_0) + i \frac{\omega_{0k}}{\omega_k} \sin \omega_k(t-t_0) \right]^2 \\
c'_2(t_{\text{in}}, t_0, t) &= \frac{g^2}{8} \int \frac{d^3\vec{k}}{(2\pi)^3} \frac{1}{\omega_{0k}^3} e^{-2i\omega_{0k}(t_0-t_{\text{in}})} \left[\cos \omega_k(t-t_0) - i \frac{\omega_{0k}}{\omega_k} \sin \omega_k(t-t_0) \right]^2 \\
c'_3(t_0, t) &= -\frac{g^2}{8} \int \frac{d^3\vec{k}}{(2\pi)^3} \frac{1}{\omega_k^2 \omega_{0k}} \left[(\cos \omega_k(t-t_0) + i \frac{\omega_{0k}}{\omega_k} \sin \omega_k(t-t_0))^2 \left(\cos 2\omega_k(t-t_0) - i \frac{(\omega_k^2 + \omega_{0k}^2)}{2\omega_k \omega_{0k}} \sin 2\omega_k(t-t_0) \right) \right. \\
&\quad \left. + \left(\cos \omega_k(t-t_0) - i \frac{\omega_{0k}}{\omega_k} \sin \omega_k(t-t_0) \right)^2 \left(\cos 2\omega_k(t-t_0) + i \frac{(\omega_k^2 + \omega_{0k}^2)}{2\omega_k \omega_{0k}} \sin 2\omega_k(t-t_0) \right) \right]. \quad (3.22)
\end{aligned}$$

In the limit of no mass quench, i.e., for $m_0 \rightarrow m$, we obtain

$$\begin{aligned}
c'_1(t_{\text{in}}, t_0, t) &\rightarrow \frac{g^2}{8} \int \frac{d^3\vec{k}}{(2\pi)^3} \frac{1}{\omega_k^3} e^{2i\omega_k(t-t_{\text{in}})}, & c'_3(t_0, t) &\rightarrow -\frac{2g^2}{8} \int \frac{d^3\vec{k}}{(2\pi)^3} \frac{1}{\omega_k^3}, \\
c'_2(t_{\text{in}}, t_0, t) &\rightarrow \frac{g^2}{8} \int \frac{d^3\vec{k}}{(2\pi)^3} \frac{1}{\omega_k^3} e^{-2i\omega_k(t-t_{\text{in}})}. \quad (3.23)
\end{aligned}$$

After evaluating all 16 correlation functions $\langle \phi_i(t) \phi_j(t) \chi_k(t_1) \chi_l(t_2) \rangle_c$ with $i, j, k, l \in \{+, -\}$, summing them and setting $\phi_+ = \phi_- = \phi$, as well as $\chi_+ = \chi_- = \chi$ to return to a description in terms of the physical fields ϕ and χ [20], we can identify the time-dependent kernel:

$$\langle \phi^2(t) \chi(t_1) \chi(t_2) \rangle_c = \underbrace{(c'_1(t_{\text{in}}, t_0, t) + c'_2(t_{\text{in}}, t_0, t))}_{K_2(t-t_0; t_0-t_{\text{in}})} \langle \chi^2(t_{\text{in}}) \chi(t_1) \chi(t_2) \rangle_c + \underbrace{c'_3(t_0, t)}_{c'_3(t-t_0)} \langle \chi^2(t) \chi(t_1) \chi(t_2) \rangle_c, \quad (3.24)$$

(ignoring terms of $\mathcal{O}(1/|\vec{k}|^5)$), we can identify the nonlocal and local kernels as:

$$\begin{aligned}
K_2(t-t_0; t_0-t_{\text{in}}) &= c'_1(t_{\text{in}}, t_0, t) + c'_2(t_{\text{in}}, t_0, t) \\
&\approx \frac{g^2}{8} \int \frac{d^3\vec{k}}{(2\pi)^3} \left[\frac{\omega_k^2 + \omega_{0k}^2}{\omega_k^2 \omega_{0k}^3} \cos(2\omega_{0k}(t_0-t_{\text{in}})) \cos(2\omega_k(t-t_0)) - \frac{1}{\omega_k \omega_{0k}^2} 2 \sin(2\omega_{0k}(t_0-t_{\text{in}})) \sin(2\omega_k(t-t_0)) \right], \quad (3.25)
\end{aligned}$$

$$c'_3 \approx -\frac{g^2}{8} \int \frac{d^3\vec{k}}{(2\pi)^3} \frac{\omega_k^2 + \omega_{0k}^2}{\omega_k^4 \omega_{0k}}. \quad (3.26)$$

Once again, the relation between the four-point correlators informs the mixing of operators weighted by local and nonlocal kernels:

$$\begin{aligned}
\phi_R^2(t) &= \phi^2(t) + K_2(t-t_0; t_0-t_{\text{in}}) \chi^2(t_{\text{in}}) \\
&\quad + c'_3 \chi^2(t) + \text{counterterms}. \quad (3.27)
\end{aligned}$$

As before, $\phi^2(t)$ arises from the disconnected diagram, with $\phi(t)$ being the bare field and counterterms are necessary to renormalize the divergence within c'_3 . The

characteristics of K_2 and details pertaining to the renormalization of c'_3 have been discussed in Sec. IV.

3. Comparison of the two cases

Using the expressions for $K_1(t-t_{\text{in}})$, c_3 , $K_2(t-t_0; t_0-t_{\text{in}})$ and c'_3 , we can conduct a straightforward comparison of the two cases while imposing various limits on t_0 , t_{in} and t . However, before doing so, the following points must be emphasized:

- (1) In case 1, the ordering $t_0 < t_{\text{in}} < t$ holds. Therefore, while we can take the limits $t \rightarrow t_{\text{in}}$ and $t_0 \rightarrow t_{\text{in}}$ separately, setting $t \rightarrow t_0$ will automatically imply that all three events, i.e., mass quench, interaction quench and the measurement are occurring at the same instant.

- (2) On the other hand, for case 2, we have the ordering $t_{\text{in}} < t_0 < t$. As a consequence, we cannot take the limit $t \rightarrow t_{\text{in}}$ directly, i.e., the limits $t \rightarrow t_0$ and $t_{\text{in}} \rightarrow t_0$ must be taken separately to describe the simultaneous occurrence of the three events.

Keeping the above points in mind, we can deduce relations between the local and nonlocal kernels and also obtain simplified forms for them.

- (1) For case 1, it is clear from Eqs. (3.17) and (3.18), that there exists a direct relation between c_3 and K_1 when we set $t \rightarrow t_{\text{in}}$ in case 1, i.e., $c_3 = -K_1(0)$. As a consequence of this, no operator mixing occurs

$$\begin{aligned} & \langle \phi^2(t)\chi(t_1)\chi(t_2) \rangle_c \\ &= (K_1(t_{\text{in}} - t_{\text{in}}) + c_3) \langle \chi^2(t_{\text{in}})\chi(t_1)\chi(t_2) \rangle_c \\ &= (K_1(0) - K_1(0)) \langle \chi^2(t_{\text{in}})\chi(t_1)\chi(t_2) \rangle_c \\ &= 0. \end{aligned} \quad (3.28)$$

This property holds irrespective of whether mass quench has occurred or not, even though $K_1(0)$ still contains a signature of the mass quench on account of the integrand being a function of both ω_k and ω_{0k} .

- (2) For case 2, while we cannot directly set $t \rightarrow t_{\text{in}}$, even if we inspect the situation where $t \rightarrow t_0$ and $t_{\text{in}} \rightarrow t_0$ hold simultaneously, we notice that $K_2(0, 0) + c'_3 \neq 0$. This turns into equality only when $\omega_k = \omega_{0k}$ is also enforced, i.e., when no mass quench occurs.
- (3) In the event of no mass quench, i.e., $m_0 = m$ and consequently $\omega_k = \omega_{0k}$, the results of [20] are reproduced for both cases:

$$\begin{aligned} K_1(t - t_{\text{in}}) &\xrightarrow{\omega_k = \omega_{0k}} K(t - t_{\text{in}}), & c_3 &\xrightarrow{\omega_k = \omega_{0k}} -K(0), \\ K_2(t - t_0; t_0 - t_{\text{in}}) &\xrightarrow{\omega_k = \omega_{0k}} K(t - t_{\text{in}}), & c'_3 &\xrightarrow{\omega_k = \omega_{0k}} -K(0). \end{aligned} \quad (3.29)$$

where time-dependent kernel is

$$K(t - t_{\text{in}}) = \frac{g^2}{4} \int \frac{d^3 \vec{k}}{(2\pi)^3} \frac{\cos(2\omega_k(t - t_{\text{in}}))}{\omega_k^3}. \quad (3.30)$$

IV. ANALYSIS OF (NON)LOCAL KERNELS

In this section we evaluate the local as well as nonlocal kernels, discussed in Sec. III, that facilitate operator mixing.

A. Numerical estimation of the kernels

Both K_1 and K_2 , see Eqs. (3.17) and (3.25), contain oscillatory functions in the integrand, weighted by momentum dependent factors. Computing these integrals

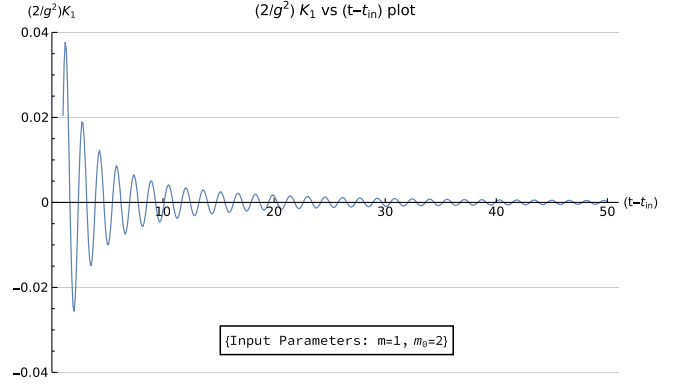


FIG. 8. Plot displaying $(2/g^2)K_1$ as a function of $(t - t_{\text{in}})$. The parameters m_0 and m have been fixed at constant values. It can be seen that K_1 vanishes at later time.

in a closed form is difficult. In [20], the kernel had been identified in terms of Meijer-G functions. In Appendix B, we have done a similar identification in terms of Meijer-G functions after doing a Taylor series expansion of the integrand assuming a small mass quench. In this section, on the other hand, we highlight the general features of K_1 and K_2 by evaluating the integrals numerically. A graphical demonstration of K_1 (scaled down by $g^2/2$) as a function of $t - t_{\text{in}}$ has been provided in Fig. 8 and highlights a decaying and oscillating profile. Similarly, K_2 (scaled down by $g^2/2$) as a function of $t - t_0$ for fixed choices of the interval $t_0 - t_{\text{in}}$ has been displayed in Fig. 9. Note that initially the nonlocal kernels exhibit “jolts” that soon equilibrate. This jolt can be ascribed to the assumption of the initial uncorrelated state, see [24] for a similar effect. One can also notice oscillatory behaviors. The different choices of $t_0 - t_{\text{in}}$ influence the location of the peak, but ultimately each of the profiles decays for large- $(t - t_0)$.

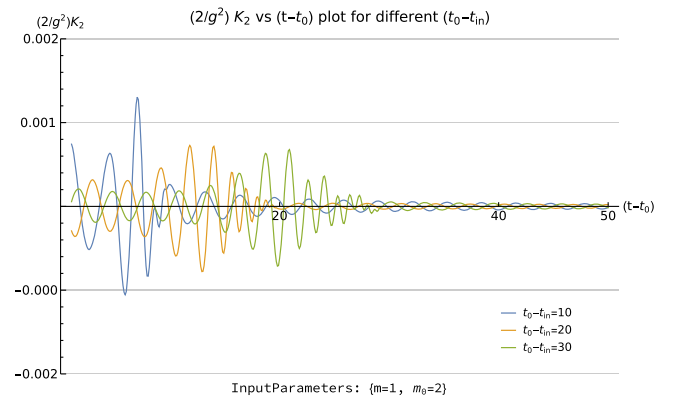


FIG. 9. Plot displaying $(2/g^2)K_2$ as a function of $(t - t_0)$ for three different choices of the interval $(t_0 - t_{\text{in}})$. The parameters m_0 and m have been fixed at constant values. Similar to K_1 , the kernel K_2 also vanishes at a later time.

B. Renormalization of divergent integrals

From Eqs. (3.18) and (3.26), it is evident that $c_3 = c'_3$. So, their features can be studied together. The integration over \vec{k} generates a logarithmic ultraviolet divergence that along with the appropriate counter-terms, see Eqs. (3.19),

(3.27), renormalizes the composite operator in both the cases. Here, c_3 and c'_3 contain divergent and finite parts. The result of evaluating the k -integral in the expression for c_3 (and c'_3), which we will denote as \tilde{c}_3 can be split based on whether $m > m_0$ or $m < m_0$ as follows:

$$\begin{aligned}\tilde{c}_3 &= -\frac{g^2}{16\pi^2} \left[\log\left(\frac{\Lambda^2}{m_0^2}\right) + \log 4 - \frac{1}{2} + \frac{1}{2\sqrt{m_0^2 - m^2}} \left(\frac{m_0^2 - 4m^2}{m}\right) \cos^{-1}\left(\frac{m}{m_0}\right) \right], \quad \text{for } m < m_0; \\ &= -\frac{g^2}{16\pi^2} \left[\log\left(\frac{\Lambda^2}{m_0^2}\right) + \log 4 - \frac{1}{2} + \frac{1}{2\sqrt{m^2 - m_0^2}} \left(\frac{m_0^2 - 4m^2}{m}\right) \cosh^{-1}\left(\frac{m}{m_0}\right) \right], \quad \text{for } m > m_0.\end{aligned}\quad (4.1)$$

Here Λ denotes the large momentum cutoff. From this complete expression, we choose the counterterms (mimicking $\overline{\text{MS}}$ scheme) judiciously by absorbing the divergent as well as the universal constant terms to ensure that operator mixing does not occur in the no mass quench limit,¹ i.e.,

$$c_3^{\text{CT}} = \tilde{c}_3(m \rightarrow m_0) = -\frac{g^2}{16\pi^2} \left[\log\left(\frac{\Lambda^2}{m_0^2}\right) + \log 4 - 2 \right]. \quad (4.2)$$

Next, the finite part of \tilde{c}_3 can be identified as $c_3^{\text{finite}} = \tilde{c}_3 - c_3^{\text{CT}}$ and the explicit form can be written as:

$$\begin{aligned}c_3^{\text{finite}} &= -\frac{g^2}{16\pi^2} \left[\frac{1}{2\sqrt{m_0^2 - m^2}} \left(\frac{m_0^2 - 4m^2}{m}\right) \cos^{-1}\left(\frac{m}{m_0}\right) + \frac{3}{2} \right], \quad \text{for } m < m_0; \\ &= -\frac{g^2}{16\pi^2} \left[\frac{1}{2\sqrt{m^2 - m_0^2}} \left(\frac{m_0^2 - 4m^2}{m}\right) \cosh^{-1}\left(\frac{m}{m_0}\right) + \frac{3}{2} \right], \quad \text{for } m > m_0.\end{aligned}\quad (4.3)$$

If we denote the change in mass after quench by Δm , i.e., if $m = m_0 + \Delta m$, then by defining a dimensionless parameter $x = -\Delta m/m_0$ and substituting $m = m_0(1 - x)$ in Eq. (4.3) we obtain,

$$\begin{aligned}c_3^{\text{finite}} &= -\frac{g^2}{16\pi^2} \left[\frac{1}{2\sqrt{x(2-x)}} \left(\frac{3-8x+4x^2}{(x-1)}\right) \cos^{-1}(1-x) + \frac{3}{2} \right], \quad \text{for } m < m_0; \\ &= -\frac{g^2}{16\pi^2} \left[\frac{1}{2\sqrt{x(x-2)}} \left(\frac{3-8x+4x^2}{(x-1)}\right) \cosh^{-1}(1-x) + \frac{3}{2} \right], \quad \text{for } m > m_0.\end{aligned}\quad (4.4)$$

It can be seen clearly that the condition ($x < 1$) must hold, otherwise m will become negative. A plot of c_3^{finite} as a function of x has been shown in Fig. 10. It can be seen from the figure that c_3^{finite} becomes largely negative as $x \rightarrow 1$, i.e., in the limit of vanishing m . The curve passing through the origin signifies the absence of operator mixing at no mass quench limit.

¹Note that for generic time dependent couplings, $\lambda(t)$, there are new counterterms proportional to derivatives of the coupling [15]. In general counter-terms involving more than one derivative of the couplings become necessary, for a comprehensive account we refer the reader to Ref. [17].

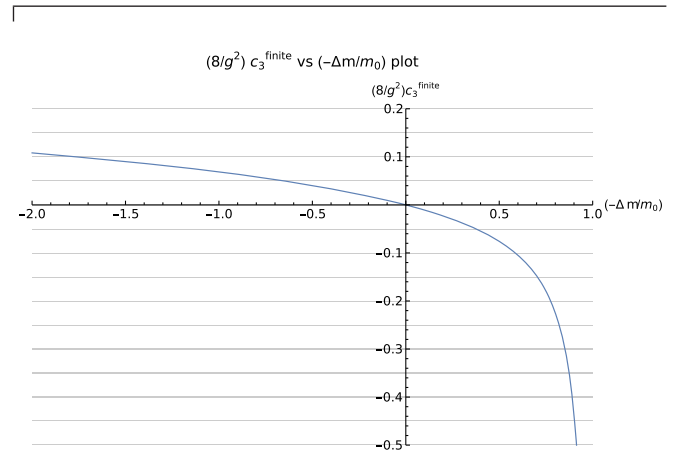


FIG. 10. Plot displaying $(8/g^2)c_3^{\text{finite}}$ as function of $x = -\Delta m/m_0$.

V. IMPLICATIONS OF OPERATOR MIXING FOR THE χ POTENTIAL

In this section, we demonstrate how the operator mixing of one field can affect the potential of other one for a two scalar field simplified system. Though the impact is mutual, we highlight the deformation of χ potential due to the $\phi^2(t)$ operator mixing. It must be mentioned that initially the χ potential is parabolic since $M^2, \lambda_\chi > 0$. We investigate, in this section, whether the $\phi^2(t)$ operator mixing can flip the sign of the χ^2 term, leading to a wine-bottle shaped potential for χ . This would imply a hint of possible phase transition or spontaneous breaking of any underlying symmetry, induced by the operator mixing, as an artifact of mass and interaction quenches. It must be emphasized that phase transitions of this nature are intricate as one is no longer limited to ground state physics.

Having obtained the operator mixing for case 1 as given in Eq. (3.19), we can substitute it back into the Lagrangian given in Eq. (3.1). The potential for the χ field, up to $\mathcal{O}(g^2)$, assumes the following form:

$$V(\chi) = \underbrace{\left(\frac{1}{2}M^2 + \frac{1}{2}m^2 c_3^{\text{finite}}\right)}_{a_1} \chi^2 + \left(\frac{1}{4!}\lambda_\chi\right)\chi^4 + \mathcal{O}(g^{2n}, n > 2). \quad (5.1)$$

Note that we have ignored the term proportional to $g^2 c_3^{\text{finite}}$ as well as the one proportional to $g^2 K_1$, as those are $\sim \mathcal{O}(g^4)$. Therefore, for boundedness of the potential we need $\lambda_\chi > 0$. Next if $a_1 > 0$ we have the usual parabolic profile of the potential. The other interesting possibility is to have $a_1 < 0$, which implies:

$$a_1 < 0 \Rightarrow (c_3^{\text{finite}} m^2 + M^2) < 0 \Rightarrow c_3^{\text{finite}} < -\frac{M^2}{m^2} \Rightarrow c_3^{\text{finite}} < -\frac{p}{(1-x)^2}, \quad (5.2)$$

where we have defined, $m = m_0(1-x)$ as earlier and $p = M^2/m_0^2$ a dimensionless parameter. Figure 11 depicts the profile of the quantity a_1 for some fixed values of p and varying x . In order to plot a_1 the values of the Lagrangian parameters g and λ_χ are kept less than unity so that perturbative expansion in terms of these parameters remains valid. The values of x and p are chosen in the anticipation of the change in the shape of the potential. So, for two choices of (x, p) , a_1 remains positive and the shape of the potential is parabolic and for the other two choices, it takes the shape of a wine-bottle. In Fig. 12, we have presented how the shape of χ potential changes for different benchmark points chosen from Fig. 11.

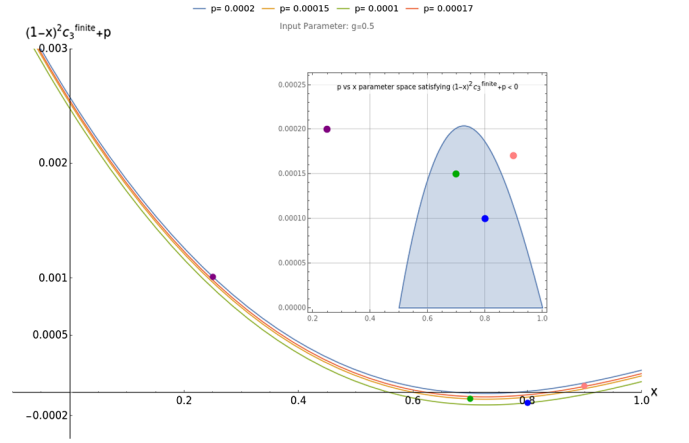


FIG. 11. Plot of $[(1-x)^2 c_3^{\text{finite}} + p]$ as a function of x and for some fixed values of p . The inset figure highlights the (x, p) parameter space that allows for negative a_1 . The points inside the shaded region correspond to potentials with the shape of a wine-bottle, those lying outside correspond to parabolic potential. Points chosen from the inset have been suitably highlighted on the main plot.

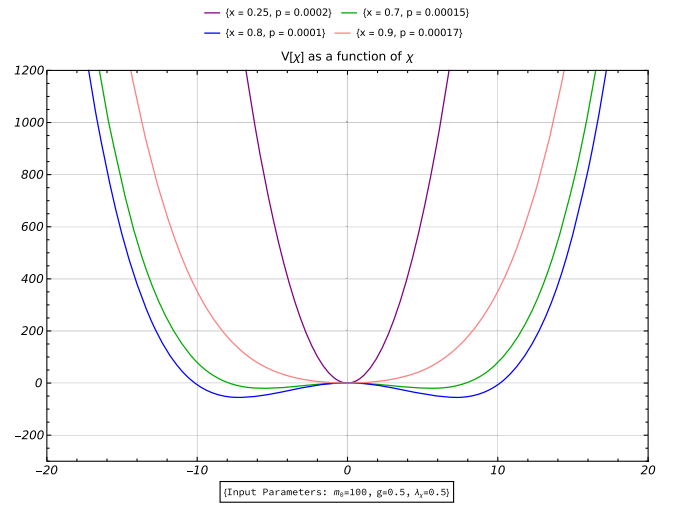


FIG. 12. Plot of $V(\chi)$ as a function of χ , for the four specific choices of x and p highlighted in Fig. 11.

VI. CONCLUSIONS AND FUTURE DIRECTIONS

In this paper we have discussed the impact of mass and interaction quenches, at times t_0 and t_{in} respectively, in operator mixing and noted its consequences on the effective potential. We computed the nonequilibrium Green's functions in the closed time path formalism, having treated the mass quench exactly in the free propagator. Our free theory computation boiled down to computing correlators analogous to that of a harmonic oscillator with time-dependent frequency. The \mathbb{Z}_2 invariant Lagrangian which we have considered, comprises of two scalar fields ϕ and χ . We have performed our analysis assuming two time

orderings: $t_0 < t_{\text{in}} \leq t < t_1 < t_2$ (interaction quench occurs after mass quench) and $t_{\text{in}} < t_0 < t < t_1 < t_2$ (mass quench occurs after interaction quench). We have estimated the $\phi^2(t)$ operator mixing for these two cases. The times t_1, t_2 are external operator times with which we find the mixings. To obtain the mixings we computed the one loop contributions to the four-point correlation function, $\langle \phi_i^2(t) \chi_j(t_1) \chi_k(t_2) \rangle$, considering all allowed diagrams and for all $i, j, k \in \{+, -\}$. All our answers depend explicitly on the quench parameters which include the changing mass of the ϕ field, the event times, t_0, t_{in} and the value of field χ at t_{in} . In the process, we have identified the time-dependent kernels ($K_{1,2}$) and mixing coefficients (c_3, c'_3). The kernels as well as the mixing coefficient contain similar UV divergences, which can be taken care of by employing suitable counterterms for both cases. The mixing of the $\phi^2(t)$ operator, at leading order in the interaction, inherits the kernel's time dependence weighted by the value of the $\chi^2(t_{\text{in}})$. More interestingly, the mixing now also contains a finite part of $c_3, c'_3 = c_3^{\text{finite}}$ weighted by the dynamical field $\chi^2(t)$. This finite piece as a function of $\Delta m = m - m_0$ grows negative and hence can flip the sign of the quadratic piece in the effective potential of χ . Therefore, the mass quench of the ϕ field can trigger the possibility of late-time phase transitions in the configuration of χ . Looking ahead, there are several interesting natural directions and possible applications that we now list.

An unresolved puzzle in the context of inflation is the continuing oscillations present in the CMB data for low multipole moments [25]. We have seen that quenches in the action can trigger memory effects in effective potentials, leading to oscillatory behaviors in time. Quench setups are natural in our expanding universe [17,26], hence it is quite conceivable that the primordial oscillations generically arise in our universe due to interacting quantum fields *out of equilibrium*.

An obvious generalization of our setup is to consider smooth quenches characterized by an amplitude and a rate. Interesting and universal scalings are known to emerge near the breakdown of adiabaticity controlled by the quench protocol [12]. We expect that the memory kernels will get imbued with characteristic scalings, that may indicate the presence of any phase transitions if present. Another generalization of the quench protocol is toward incorporating multiple quenches whose physics is quite different

than a single quench [27]. In particular, thermalization can occur exponentially fast and the integrable nature of a system gets washed out very quickly.

The discussion of symmetries itself becomes complicated *out of equilibrium* as the dynamics is no longer confined to the ground state.² This is closely tied with the generation of an effective thermalization of the system, that can, in most cases, explicitly restore spontaneously broken symmetries, see however [28]. The connection with quenches comes via the eigenstate thermalization hypothesis [29] which posits that every finite density energy eigenstate is approximately thermal. Any *out of equilibrium* scenario necessarily involves excited states, hence it is natural that an interacting system may effectively thermalize.

Finally, to draw the correct physics lessons, we need to go beyond perturbative methods. This may be possible in large N theories when the system becomes exactly solvable. Recently, [30,31] have resummed loop contributions to the *in-in* correlators using the Weisskopf-Wigner method. It will be important to use this tool in our setup to find the nonperturbative results in time dependence.

ACKNOWLEDGMENTS

D. D. and B. D. would like to acknowledge the support provided by the Max Planck Partner Group Grant No. MAXPLA/PHY/2018577. D. D. would also like to acknowledge the support provided by the MATRICS Grant No. SERB/PHY/2020334. B. D. also acknowledges MHRD, Government of India for Research Fellowship. The work of J. C. and S. U. R. is supported by the Science and Engineering Research Board, Government of India, under the Agreement No. SERB/PHY/2019501 (MATRICS). S. P. is supported by the MHRD, Government of India, under the Prime Minister's Research Fellows (PMRF) Scheme, 2020.

APPENDIX A: DETAILS OF LOOP CALCULATIONS

The contribution from the one-loop diagrams of Fig. 5 (L_1 and L_2), as well as the additional diagrams (L'_1 and L'_2) obtained on exchanging \vec{p}_1 and \vec{p}_2 , to the four-point correlation function $\langle \phi_+^2(t) \chi_+(t_1) \chi_+(t_2) \rangle_c$ can be expressed as the following integrals:

$$L_1 + L'_1 = 2 \times \frac{-ig^2}{2} \int \frac{d^3\vec{k}}{(2\pi)^3} \int_{t_{\text{in}}}^{\infty} d\tau [G_{++}^{\phi}(\vec{k}, t, \tau) G_{++}^{\phi}(\vec{P} - \vec{k}, t, \tau) G_{++}^{\chi}(\vec{p}_1, \tau, t_1) G_{++}^{\chi}(\vec{p}_2, \tau, t_2)] + (\vec{p}_1 \leftrightarrow \vec{p}_2), \quad (\text{A1})$$

$$L_2 + L'_2 = 2 \times \frac{ig^2}{2} \int \frac{d^3\vec{k}}{(2\pi)^3} \int_{t_{\text{in}}}^{\infty} d\tau [G_{+-}^{\phi}(\vec{k}, t, \tau) G_{+-}^{\phi}(\vec{P} - \vec{k}, t, \tau) G_{+-}^{\chi}(\vec{p}_1, \tau, t_1) G_{+-}^{\chi}(\vec{p}_2, \tau, t_2)] + (\vec{p}_1 \leftrightarrow \vec{p}_2). \quad (\text{A2})$$

²The ground state characterizes the equilibrium phase of matter.

The nontrivial form of the Green's functions of the ϕ field, due to the sudden quench of its mass, makes it difficult to evaluate these integrals. The full expansion of the integrand, after multiplication of the terms within the Green's functions, leads to a large number of terms but the presence of θ -functions, see Eqs. (3.6) and (3.10), splits the full integral into multiple pieces with various limits of integration and one can then write,

For case 1:

$$\begin{aligned}
L_1 + L'_1 = & 2 \times \frac{-ig^2}{2} \int \frac{d^3\vec{k}}{(2\pi)^3} \left[\int_{t_{\text{in}}}^t d\tau \frac{e^{i\Omega_{p_1}(\tau-t_1)}}{2\Omega_{p_1}} \frac{e^{i\Omega_{p_2}(\tau-t_2)}}{2\Omega_{p_2}} u_{\text{in}}(\vec{k}, t) u_{\text{in}}(\vec{P}-\vec{k}, t) u_{\text{in}}^*(\vec{k}, \tau) u_{\text{in}}^*(\vec{P}-\vec{k}, \tau) \right. \\
& + \int_t^{t_1} d\tau \frac{e^{i\Omega_{p_1}(\tau-t_1)}}{2\Omega_{p_1}} \frac{e^{i\Omega_{p_2}(\tau-t_2)}}{2\Omega_{p_2}} u_{\text{in}}(\vec{k}, \tau) u_{\text{in}}(\vec{P}-\vec{k}, \tau) u_{\text{in}}^*(\vec{k}, t) u_{\text{in}}^*(\vec{P}-\vec{k}, t) \\
& + \int_{t_1}^{t_2} d\tau \frac{e^{-i\Omega_{p_1}(\tau-t_1)}}{2\Omega_{p_1}} \frac{e^{i\Omega_{p_2}(\tau-t_2)}}{2\Omega_{p_2}} u_{\text{in}}(\vec{k}, \tau) u_{\text{in}}(\vec{P}-\vec{k}, \tau) u_{\text{in}}^*(\vec{k}, t) u_{\text{in}}^*(\vec{P}-\vec{k}, t) \\
& \left. + \int_{t_2}^{\infty} d\tau \frac{e^{-i\Omega_{p_1}(\tau-t_1)}}{2\Omega_{p_1}} \frac{e^{-i\Omega_{p_2}(\tau-t_2)}}{2\Omega_{p_2}} u_{\text{in}}(\vec{k}, \tau) u_{\text{in}}(\vec{P}-\vec{k}, \tau) u_{\text{in}}^*(\vec{k}, t) u_{\text{in}}^*(\vec{P}-\vec{k}, t) \right] + (\vec{p}_1 \leftrightarrow \vec{p}_2), \quad (\text{A3})
\end{aligned}$$

$$L_2 + L'_2 = 2 \times \frac{ig^2}{2} \int \frac{d^3\vec{k}}{(2\pi)^3} \left[\int_{t_{\text{in}}}^{\infty} d\tau \frac{e^{-i\Omega_{p_1}(\tau-t_1)}}{2\Omega_{p_1}} \frac{e^{-i\Omega_{p_2}(\tau-t_2)}}{2\Omega_{p_2}} u_{\text{in}}(\vec{k}, \tau) u_{\text{in}}(\vec{P}-\vec{k}, \tau) u_{\text{in}}^*(\vec{k}, t) u_{\text{in}}^*(\vec{P}-\vec{k}, t) \right] + (\vec{p}_1 \leftrightarrow \vec{p}_2). \quad (\text{A4})$$

For case 2:

$$\begin{aligned}
L_1 + L'_1 = & 2 \times \frac{-ig^2}{2} \int \frac{d^3\vec{k}}{(2\pi)^3} \left[\int_{t_{\text{in}}}^{t_0} d\tau \frac{e^{2i\omega_{0k}(\tau-t_0)}}{2\omega_{0k}} \frac{e^{i\Omega_{p_1}(\tau-t_1)}}{2\Omega_{p_1}} \frac{e^{i\Omega_{p_2}(\tau-t_2)}}{2\Omega_{p_2}} u_{\text{in}}(\vec{k}, t) u_{\text{in}}(\vec{P}-\vec{k}, t) \right. \\
& + \int_{t_0}^t d\tau \frac{e^{i\Omega_{p_1}(\tau-t_1)}}{2\Omega_{p_1}} \frac{e^{i\Omega_{p_2}(\tau-t_2)}}{2\Omega_{p_2}} u_{\text{in}}(\vec{k}, t) u_{\text{in}}(\vec{P}-\vec{k}, t) u_{\text{in}}^*(\vec{k}, \tau) u_{\text{in}}^*(\vec{P}-\vec{k}, \tau) \\
& + \int_t^{t_1} d\tau \frac{e^{i\Omega_{p_1}(\tau-t_1)}}{2\Omega_{p_1}} \frac{e^{i\Omega_{p_2}(\tau-t_2)}}{2\Omega_{p_2}} u_{\text{in}}(\vec{k}, \tau) u_{\text{in}}(\vec{P}-\vec{k}, \tau) u_{\text{in}}^*(\vec{k}, t) u_{\text{in}}^*(\vec{P}-\vec{k}, t) \\
& + \int_{t_1}^{t_2} d\tau \frac{e^{-i\Omega_{p_1}(\tau-t_1)}}{2\Omega_{p_1}} \frac{e^{i\Omega_{p_2}(\tau-t_2)}}{2\Omega_{p_2}} u_{\text{in}}(\vec{k}, \tau) u_{\text{in}}(\vec{P}-\vec{k}, \tau) u_{\text{in}}^*(\vec{k}, t) u_{\text{in}}^*(\vec{P}-\vec{k}, t) \\
& \left. + \int_{t_2}^{\infty} d\tau \frac{e^{-i\Omega_{p_1}(\tau-t_1)}}{2\Omega_{p_1}} \frac{e^{-i\Omega_{p_2}(\tau-t_2)}}{2\Omega_{p_2}} u_{\text{in}}(\vec{k}, \tau) u_{\text{in}}(\vec{P}-\vec{k}, \tau) u_{\text{in}}^*(\vec{k}, t) u_{\text{in}}^*(\vec{P}-\vec{k}, t) \right] + (\vec{p}_1 \leftrightarrow \vec{p}_2), \quad (\text{A5})
\end{aligned}$$

$$\begin{aligned}
L_2 + L'_2 = & 2 \times \frac{ig^2}{2} \int \frac{d^3\vec{k}}{(2\pi)^3} \left[\int_{t_{\text{in}}}^{t_0} d\tau \frac{e^{-2i\omega_{0k}(\tau-t_0)}}{2\omega_{0k}} \frac{e^{-i\Omega_{p_1}(\tau-t_1)}}{2\Omega_{p_1}} \frac{e^{-i\Omega_{p_2}(\tau-t_2)}}{2\Omega_{p_2}} u_{\text{in}}^*(\vec{k}, t) u_{\text{in}}^*(\vec{P}-\vec{k}, t) \right. \\
& \left. + \int_{t_0}^{\infty} d\tau \frac{e^{-i\Omega_{p_1}(\tau-t_1)}}{2\Omega_{p_1}} \frac{e^{-i\Omega_{p_2}(\tau-t_2)}}{2\Omega_{p_2}} u_{\text{in}}(\vec{k}, \tau) u_{\text{in}}(\vec{P}-\vec{k}, \tau) u_{\text{in}}^*(\vec{k}, t) u_{\text{in}}^*(\vec{P}-\vec{k}, t) \right] + (\vec{p}_1 \leftrightarrow \vec{p}_2). \quad (\text{A6})
\end{aligned}$$

For both case 1 and case 2, the total contribution to the correlation function is obtained after summing up $L_1 + L'_1 + L_2 + L'_2$. Eqs. (A3)–(A6) are further simplified by appropriately substituting for u_{in} , u_{in}^* using Eq. (3.7) and by working in a large- \vec{k} limit which implies: $(\vec{P}-\vec{k})^2 + m^2 \approx \vec{k}^2 + m^2$. Subsequently, the integration over τ can be done using computational tools such as *Mathematica* [32]. After the integration, the result can be

further filtered by keeping only the leading and subleading powers of \vec{k} in the numerator as well as the denominator. Finally, ignoring all terms except the ones of the order $1/|\vec{k}|^3$, we can identify four-point correlation functions of χ along with their time-dependent coefficients. This procedure ultimately leads to the contents of Eqs. (3.11) and (3.20) for case 1 and case 2 respectively.

APPENDIX B: SERIES EXPANSION OF THE KERNELS FOR SMALL MASS QUENCH

Expansion of the postquench mass of the ϕ field (m) around the prequench mass (m_0) as $m = m_0 + \delta m$, assuming a small δm , leads to the following relation between ω_k and ω_{0k} :

$$\omega_k = \omega_{0k} + \delta\omega_k \quad \text{with} \quad \delta\omega_k = \frac{m_0}{\omega_{0k}} \delta m.$$

Based on this, the kernels K_1 and c_3 , defined in Eqs. (3.17) and (3.18), respectively, can also be expanded, up to linear order in δm as:

$$\begin{aligned} K_1(t-t_{\text{in}}; t_{\text{in}}-t_0) &= \frac{g^2}{4} \int \frac{d^3\vec{k}}{(2\pi)^3} \frac{\cos 2\omega_{0k}(t-t_{\text{in}})}{\omega_{0k}^3} - \frac{g^2 m_0}{4} \delta m \left[3 \int \frac{d^3\vec{k}}{(2\pi)^3} \frac{\cos 2\omega_{0k}(t-t_{\text{in}})}{\omega_{0k}^5} + 2 \int \frac{d^3\vec{k}}{(2\pi)^3} (t-t_{\text{in}}) \frac{\sin 2\omega_{0k}(t-t_{\text{in}})}{\omega_{0k}^4} \right] \\ &= \frac{g^2}{32\pi} G_{1,3}^{2,0}(z^2|_{0,0,1/2}^{3/2}) - \frac{g^2 \delta m}{32\pi m_0} \left[3G_{1,3}^{2,0}(z^2|_{1,0,1/2}^{5/2}) - z \frac{d}{dz} [G_{1,3}^{2,0}(z^2|_{1,0,1/2}^{5/2})] \right], \end{aligned} \quad (\text{B1})$$

$$\begin{aligned} c_3(t, t_0) &= -\frac{g^2}{4} \int \frac{d^3\vec{k}}{(2\pi)^3} \frac{1}{\omega_{0k}^3} + \frac{3m_0 g^2}{4} \int \frac{d^3\vec{k}}{(2\pi)^3} \frac{1}{\omega_{0k}^5} \delta m \\ &= -\frac{g^2}{8\pi^2} \left[-\frac{\Lambda}{\sqrt{\Lambda^2 + m_0^2}} + \log \left(\frac{\Lambda}{m_0} + \sqrt{1 + \frac{\Lambda^2}{m_0^2}} \right) \right] + \frac{g^2}{8\pi^2 m_0} \delta m, \end{aligned} \quad (\text{B2})$$

where, $z = m_0(t-t_{\text{in}})$, with m_0 assumed to be a constant and Λ is the UV cutoff. It must be noted that the zeroth order term is the same as what was reported in [20].

For case 2, the kernels K_2 and c'_3 , see Eqs. (3.25) and (3.26), can similarly be expanded:

$$\begin{aligned} K_2(t-t_{\text{in}}; t_{\text{in}}-t_0) &= \frac{g^2}{4} \int \frac{d^3\vec{k}}{(2\pi)^3} \frac{\cos 2\omega_{0k}(t-t_{\text{in}})}{\omega_{0k}^3} - \frac{m_0 \delta m g^2}{4} \left[\int \frac{d^3\vec{k}}{(2\pi)^3} \frac{\cos 2\omega_{0k}(t-t_{\text{in}})}{\omega_{0k}^5} + \int \frac{d^3\vec{k}}{(2\pi)^3} 2(t-t_0) \frac{\sin 2\omega_{0k}(t-t_{\text{in}})}{\omega_{0k}^4} \right] \\ &= \frac{g^2}{32\pi} G_{1,3}^{2,0}(z^2|_{0,0,1/2}^{3/2}) - \frac{\delta m g^2}{32\pi m_0} \left[G_{1,3}^{2,0}(z^2|_{1,0,1/2}^{5/2}) - z \frac{d}{dz} [G_{1,3}^{2,0}(z^2|_{1,0,1/2}^{5/2})] + (t_{\text{in}}-t_0) \frac{d}{dz} [G_{1,3}^{2,0}(z^2|_{1,0,1/2}^{5/2})] \right], \end{aligned} \quad (\text{B3})$$

$$\begin{aligned} c'_3(t, t_0) &= -\frac{g^2}{4} \int \frac{d^3\vec{k}}{(2\pi)^3} \frac{1}{\omega_{0k}^3} + \frac{3m_0 g^2}{4} \int \frac{d^3\vec{k}}{(2\pi)^3} \frac{1}{\omega_{0k}^5} \delta m \\ &= -\frac{g^2}{8\pi^2} \left[-\frac{\Lambda}{\sqrt{\Lambda^2 + m_0^2}} + \log \left(\frac{\Lambda}{m_0} + \sqrt{1 + \frac{\Lambda^2}{m_0^2}} \right) \right] + \frac{g^2}{8\pi^2 m_0} \delta m. \end{aligned} \quad (\text{B4})$$

The \vec{k} -integrals within each of these expressions can be rewritten in terms of Meijer-G functions. In Table I, we have listed the relevant Meijer-G functions and their asymptotic functional forms.

TABLE I. Meijer-G functions corresponding to the integrals present in the Kernel definitions, along with their asymptotic limits. For the limiting cases, we have only reported the first nonzero term of the series expansion. Here, $z = m_0(t-t_{\text{in}})$.

Meijer-G function	Large z limit	Small z -limit
$G_{1,3}^{2,0}(z^2 _{0,0,1/2}^{3/2})$	$-\frac{z^{-3/2}}{\sqrt{2\pi}} (\cos(2z) + \sin(2z))$	$-\frac{4}{\pi} (1 + \gamma_E + \log(z))$
$G_{1,3}^{2,0}(z^2 _{1,0,1/2}^{5/2})$	$-\frac{z^{-3/2}}{\sqrt{2\pi}} (\cos(2z) + \sin(2z))$	$\frac{4}{3\pi}$
$\frac{d}{dz} [G_{1,3}^{2,0}(z^2 _{1,0,1/2}^{5/2})]$	$-2 \frac{z^{-3/2}}{\sqrt{2\pi}} (\cos(2z) - \sin(2z))$	$\frac{16z}{\pi} (\gamma_E + \log(z))$

- [1] E. A. Calzetta and B.-L. B. Hu, *Nonequilibrium Quantum Field Theory*, Cambridge Monographs on Mathematical Physics (Cambridge University Press, Cambridge, England, 2008).
- [2] P. Millington, *Thermal Quantum Field Theory and Perturbative Non-Equilibrium Dynamics* (Springer Science & Business Media, Berlin, Heidelberg, 2013).
- [3] T. W. B. Kibble, Topology of cosmic domains and strings, *J. Phys. A* **9**, 1387 (1976).
- [4] W. H. Zurek, Cosmological experiments in superfluid helium?, *Nature (London)* **317**, 505 (1985).
- [5] S. R. Das, D. A. Galante, and R. C. Myers, Universality in fast quantum quenches, *J. High Energy Phys.* **02** (2015) 167.
- [6] S. R. Das, D. A. Galante, and R. C. Myers, Universal Scaling in Fast Quantum Quenches in Conformal Field Theories, *Phys. Rev. Lett.* **112**, 171601 (2014).
- [7] S. R. Das, D. A. Galante, and R. C. Myers, Smooth and fast versus instantaneous quenches in quantum field theory, *J. High Energy Phys.* **08** (2015) 073.
- [8] S. R. Das, D. A. Galante, and R. C. Myers, Quantum quenches in free field theory: Universal scaling at any rate, *J. High Energy Phys.* **05** (2016) 164.
- [9] D. Das, S. R. Das, D. A. Galante, R. C. Myers, and K. Sengupta, An exactly solvable quench protocol for integrable spin models, *J. High Energy Phys.* **11** (2017) 157.
- [10] S. R. Das and K. Sengupta, Non-equilibrium dynamics of $O(N)$ nonlinear sigma models: A large- N approach, *J. High Energy Phys.* **09** (2012) 72.
- [11] D. Das and B. Dey, Quantum quench, large N , and symmetry restoration, *J. High Energy Phys.* **07** (2020) 107.
- [12] S. R. Das, Old and new scaling laws in quantum quench, *Prog. Theor. Exp. Phys.* **2016**, 12C107 (2016).
- [13] A. Dymarsky and M. Smolkin, Universality of fast quenches from the conformal perturbation theory, *J. High Energy Phys.* **01** (2018) 112.
- [14] R. D. Jordan, Effective field equations for expectation values, *Phys. Rev. D* **33**, 444 (1986).
- [15] M. Goykhman, T. Shachar, and M. Smolkin, On quantum quenches at one loop, *J. High Energy Phys.* **01** (2019) 022.
- [16] L. S. Brown and J. C. Collins, Dimensional renormalization of scalar field theory in curved space-time, *Ann. Phys. (N.Y.)* **130**, 215 (1980).
- [17] N. D. Birrell and P. C. W. Davies, *Quantum Fields in Curved Space*, Cambridge Monographs on Mathematical Physics (Cambridge University Press, Cambridge, England, 1984).
- [18] D. J. Toms, Renormalization of interacting scalar field theories in curved space-time, *Phys. Rev. D* **26**, 2713 (1982).
- [19] E. Calzetta and B. L. Hu, Closed-time-path functional formalism in curved spacetime: Application to cosmological back-reaction problems, *Phys. Rev. D* **35**, 495 (1987).
- [20] S. Dresti and A. Riotto, Renormalization of composite operators in time-dependent backgrounds, *Nucl. Phys.* **B874**, 792 (2013).
- [21] C. Burrage, C. Käding, P. Millington, and J. Mináf, Open quantum dynamics induced by light scalar fields, *Phys. Rev. D* **100**, 076003 (2019).
- [22] S. Sotiriadis and J. Cardy, Quantum quench in interacting field theory: A self-consistent approximation, *Phys. Rev. B* **81**, 134305 (2010).
- [23] Y. BenTov, Schwinger-Keldysh path integral for the quantum harmonic oscillator, [arXiv:2102.05029](https://arxiv.org/abs/2102.05029).
- [24] B. L. Hu, J. P. Paz, and Y. Zhang, Quantum Brownian motion in a general environment: Exact master equation with nonlocal dissipation and colored noise, *Phys. Rev. D* **45**, 2843 (1992).
- [25] M. Aich, D. K. Hazra, L. Sriramkumar, and T. Souradeep, Oscillations in the inflaton potential: Complete numerical treatment and comparison with the recent and forthcoming CMB datasets, *Phys. Rev. D* **87**, 083526 (2013).
- [26] L. Covi and S. Dresti, Time-dependent features in the primordial spectrum, [arXiv:1803.02351](https://arxiv.org/abs/1803.02351).
- [27] S. Ghosh, K. S. Gupta, and S. C. L. Srivastava, Exact Relaxation Dynamics and Quantum Information Scrambling in Multiply Quenched Harmonic Chains, *Phys. Rev. E* **100**, 012215 (2019).
- [28] N. Chai, S. Chaudhuri, C. Choi, Z. Komargodski, E. Rabinovici, and M. Smolkin, Symmetry Breaking at All Temperatures, *Phys. Rev. Lett.* **125**, 131603 (2020).
- [29] M. Srednicki, Chaos and quantum thermalization, *Phys. Rev. E* **50**, 888 (1994).
- [30] S. Chaykov, N. Agarwal, S. Bahrami, and R. Holman, Loop corrections in Minkowski spacetime away from equilibrium 1: Late-time resummations, [arXiv:2206.11288](https://arxiv.org/abs/2206.11288).
- [31] S. Chaykov, N. Agarwal, S. Bahrami, and R. Holman, Loop corrections in Minkowski spacetime away from equilibrium 2: Finite-time results, [arXiv:2206.11289](https://arxiv.org/abs/2206.11289).
- [32] W. R. Inc., *Mathematica*, Version 13.1. Champaign, IL, 2022.